Supplemental Material of

Anaerobic digestion of sludge by different pretreatments: Changes of amino acids and microbial community

Keke Xiao[a,b], Zecong Yu[a,b], Kangyue Pei[a,b], Mei Sun[a,b], Yuwei Zhu[a,b], Sha Liang[a,b], Huijie Hou[a,b], Bingchuan Liu[a,b], Jingping Hu[a,b], Jiakuan Yang[a,b,c,*]

[a] *School of Environmental Science and Engineering, Huazhong University of Science and Technology, Luoyu Road 1037, Wuhan, Hubei, 430074, China*

[b] *Hubei Provincial Engineering Laboratory of Solid Waste Treatment, Disposal and Recycle Technology, Luoyu Road 1037, Wuhan, Hubei, 430074, China*

[c] *State Key Laboratory of Coal Combustion, Huazhong University of Science and Technology, Luoyu Road 1037, Wuhan, Hubei, 430074, China*

*Corresponding author

* Prof. Jiakuan Yang

Tel: +86-27-87792102, Fax: +86-27-87792101.

E-mail addresses: jkyang@mail.hust.edu.cn; yjiakuan@hotmail.com (J. K. Yang).

Number of pages: 27

Number of Texts: 2

Number of Tables: 7

Number of Figures: 6

Contents of Supporting Information

Text S1 Sludge source and characteristics

The Sanjintan wastewater treatment plant treated municipal wastewater using an anaerobic−oxic process, at a flow rate of 300,000 m^3/d. The influent of Shahu wastewater treatment plant is mainly municipal wastewater, and its treatment process is anaerobic−anoxic−aerobic, at a flow rate of 100,000 m^3/d. The characteristics of the raw feed sludge and seed sludge are listed in **Table S1**.

Text S2 Analytical methods

The measurements of TS, VS, SCOD and NH_4^+-N followed the methods described in standard methods (APHA, 2005). A pH meter purchased from Mettler-Toledo (S220, Germany) was used for pH measurement. ORP was measured by an ORP electrode (MTC301, Hach Instrument Co., Ltd, USA). The concentration of VFAs was measured with a gas chromatography (GC9790Plus, Fuli, China), equipped with a flame ionized detector. A pressure meter (Dwyer 490, Indiana, USA) was used to calculate the biogas volume, and the composition of biogas was measured with a gas chromatography (GC9790Plus, Fuli, China), equipped with a thermal conductivity detector. The protein concentration was determined with a Lowry method using a commercial kit (Xiao et al., 2017). The concentration of polysaccharide was measured with phenol-sulphuric acid method (Xiao et al., 2016).

Sludge samples were centrifuged with a low temperature and high-speed centrifuge (Hengnuo, China) at 4 ºC (4000 *g*, 10 minutes). The supernatant was obtained as the liquid phase. The changes

of protein conformation in the liquid phase of different sludge samples before and after anaerobic digestion were monitored with a Fourier transform infrared spectroscopy (FTIR) instrument (Bruker Vertex 80, America). Prior to analysis, the sludge supernatant was freeze-dried with a freeze dryer (Boyikang, China) for 36 h to obtain a dry powder sample. Then 10 mg powder sample was mixed with potassium bromide (a mass ratio of 1:100). The operational parameters of the FTIR instrument were as follows: A frequency range of 4000 to 600 cm^{-1}, scan numbers of 32, and a scan resolution of 4 cm^{-1}. For the determination of the protein secondary structure, the amide I region of protein, namely at the spectrum of 1700-1600 cm^{-1}, was deconvoluted with a Gaussian cure fitting based on a nine-point Savitzky-Golay derivative function using a PEAKFIT v4.12 software.

To investigate protein type, three-dimensional excitation emission matrix fluorescence spectroscopy was conducted. The emission wavelength ranged from 250 to 550 nm at a 5 nm sampling interval, and the excitation wavelength ranged from 200 to 450 nm at a 5 nm sampling interval. The spectra were recorded with the operational parameters as follows: 12,000 nm/min scan rate, and slit bandwidths for excitation (Ex) and emission (Em) were both 5 nm. Based on the definition in You et al. (2017), the 3D-EEM spectra are categorized into five regions: Tryptophan-like protein (Ex: 250-400 nm; Em : 280-380 nm), aromatic protein I (Ex: 200-250 nm; Em: 280-380 nm), aromatic protein II (Ex: 200-250 nm; Em: 280-380 nm), humic acid (Ex: 250-400; Em: >380 nm), and fulvic acid (Ex: 200-250 nm; Em: >380 nm).

A simple and direct pre-column derivatization method using high performance liquid chromatography (HPLC) was adopted for the analysis of amino acids, and details of which can be found in Le and Stuckey (2017). Briefly, sludge samples were firstly centrifuged at 4000 *g* for 10 minutes to obtain the sludge supernatant. And then sludge supernatant was lyophilized in a freeze

dryer (Boyikang, China) for 5 days to obtain a dry powder sample. The freeze-dried samples were subsequently dissolved in 0.1 mol/L of hydrochloric acid, and were exposed to amino acids analysis using HPLC (Agilent 1260, USA) equipped with an ultra-violet diode array detector and an Agilent Zorbax Eclipse Plus C18 column.

ATP was measured with a commercial BacTiter-Glo™ kit (Promega, USA). The sludge samples were firstly diluted with 1 × phosphate buffered saline buffer (pH of 7.4) to ensure the samples could be interpolated within the standard curve. Subsequently, 100 μL specific commercial reagent and 100 μL sludge samples were incubated on opaque-walled 96-well plates on an orbital shaker for 5 minutes. The luminescence data was recorded with a plate reader (Mithras LB940, Germany). The specific ATP concentration was normalized against VS concentration.

To investigate the kinetic parameters of methane production process for each sludge sample, the cumulative methane production was fitted to a modified Gompertz model as follows (Li et al., 2019):

$$M(t) = P \times \exp\left(-\exp\left[\frac{Rmax \times e}{P} \times (\lambda - t) + 1\right]\right)$$

where M(t) denotes the cumulative methane production (mL) at time t (h); P denotes the maximum yield of methane (mL); R_{max} denotes the maximum methane production rate (mL/h); e denotes exponential constant; λ denotes the lag phase (h).

Both high-throughput and metagenomic sequencing analyses were conducted to understand the changes of microbial communities. In brief, DNA extraction and 16S rRNA sequencing analysis were conducted to investigate the taxonomic patterns of microbial community. DNA was extracted using a magnetic soil and stool DNA kit (Tiangen Biotech, Beijing, China). The 16S rRNA gene universal bacterial primer set of 341 F (CCTACGGGRBGCASCAG) and 806 R

(GGACTACNNGGGTATCTAAT), targeting V3 − V4 hypervariable region (Berg et al., 2012) and 16S rRNA gene universal archaeal primer set of 519F (CAGCCGCCGCGGTAA) and 915R (GTGCTCCCCCGCCAATTCCT), targeting V4 – V5 hypervariable region were used for amplification (Fei et al., 2015). The pyrosequencing analysis of DNA samples was conducted by Novogene (Beijing, China). In brief, according to the characteristics of the amplified region, based on the IonS5^{TM}XL sequencing platform, single-end sequencing is used to construct a library by sorting, trimming and screening the raw data. The clean sequences were then clustered into operational taxonomic units (OTUs) by filtering, followed by species annotation and abundance analysis. Further alpha diversity analysis and beta diversity analysis were conducted, and rarefaction curves were constructed.

Prior to library construction for metagenomic sequencing, samples were tested with final optical density (OD) value between 1.8 − 2.0. Sequencing libraries were generated using NEBNext® Ultra™ DNA Library Prep Kit for Illumina (NEB, USA) following manufacturer's recommendations and index codes were added to attribute sequences to each sample. The clustering of the index-coded samples was performed on a cBot Cluster Generation System according to the manufacturer's instructions. After cluster generation, the library preparations were sequenced on an Illumina HiSeq platform (Illumina Novaseq6000, PE150) and paired-end reads were generated. For metagenomic analysis, steps like sequencing results pretreatment, metagenome assembly, gene prediction and abundance analysis, taxonomy prediction, common functional database annotations, and resistance gene annotation were conducted. In brief, preprocessing the raw data obtained from the Illumina HiSeq sequencing platform using Readfq (V8, https://github.com/cjfields/readfq) was conducted to acquire the Clean Data for subsequent analysis. The specific processing steps were as

follows: a) remove the reads which contain low quality bases (default quality threshold value ≤ 38) above a certain portion (default length of 40 bp); b) remove the reads in which the N base has reached a certain percentage (default length of 10 bp); c) remove reads which shared the overlap above a certain portion with Adapter (default length of 15 bp) (Handelsman et al., 1998). The Clean Data were then blasted using Bowtie2.2.4 software (Bowtie2.2.4, http://bowtie-bio.sourceforge.net/bowtie2/index.shtml) to filter the reads that are of host origin with parameters as follows: end to end; sensitive, I 200, and X 400 (Tringe and Rubin, 2005). The fragment shorter than 500 bp in all of Scaftigs for statistical analysis both generated from single or mixed assembly was then filtered (Tringe et al., 2005). The Scaftigs (≥ 500 bp) were all predicted the ORF by MetaGeneMark (V2.10, http://topaz.gatech.edu/GeneMark/) software, and the length information shorter than 100 nt was filtered from the predicted result with default parameters (Feng et al., 2015). DIAMOND software (V0.9.9) was used for taxonomy prediction and common functional database annotations (Nielsen et al., 2014). Functional database include KEGG database (Version 2018-01-01, http://www.kegg.jp/kegg/) (Kanehisa et al., 2006; Kanehisa et al., 2013), eggNOG database (Version 4.5, http://eggnogdb.embl.de/#/app/home) (Powell et al., 2014), Carbohydrate-Active EnZymes (CAZy) database (Version 201801, http://www.cazy.org/) (Cantarel et al., 2009). For the blast result of each sequence, the best Blast Hit is used for subsequent analysis (Li et al., 2014; Bäckhed et al., 2015; Feng et al., 2015). Resistance Gene Identifier (RGI) software was used to align the Unigenes to CARD database (https://card.mcmaster.ca/) (Karlsson et al., 2012).

Pearson's correlation coefficients were determined by Statistical Product and Service Solutions (SPSS) 19.0 software. The structural equation model (SEM) is a multivariate statistical framework used to estimate, investigate, and examine the causal relationship between independent and

dependent variables (Zong et al., 2019). The SEM model was performed using SPSS and Amos Graphics Software. The principal component analysis was conducted with the Statistical Analysis System (SAS) 8.0. An analysis of variance (ANOVA) was used to indicate the significance of results, and probability (p) value less than 0.05 was regarded as statistically significant.

Table S1. The characteristics of the feed sludge and seed sludge.

Sludge sample	Water content (%)	pH	TS (g/L)	VS (g/L)	CST (s)	SRF (10^{13} m/kg)	SCOD (mg/L)	ORP (mV)	Total protein (mg/L)	Total polysaccharide (mg/L)	NH_4^+-N (mg/L)
Feed	96.78 ± 0.86	6.83 ± 0.12	32.82 ± 1.22	14.57 ± 0.02	154.2 ± 2.5	1.66 ± 1.22	296.3 ± 5.1	−278.67 ± 3.41	150.51 ± 4.64	32.16 ± 0.73	190.25 ± 2.01
Seed	95.85 ± 0.94	6.92 ± 0.22	41.05 ± 1.25	15.49 ± 0.72	221.2 ± 4.4	2.12 ± 2.68	428.3 ± 4.4	−298.77 ± 5.42	84.21 ± 3.59	29.54 ± 1.67	490.25 ± 2.01

Noted: CST denotes capillary suction time; Feed denotes waste activated sludge drawn from the Shahu wastewater treatment plants, without any pretreatment; ORP denotes oxidation reduction potential; Seed denotes anaerobic digestion sludge obtained from the Sanjintan wastewater treatment plants, without any pretreatment; SRF denotes specific resistance to filtration; SCOD denotes soluble chemical oxygen demand; TS denotes total solids; VS denotes volatile solids.

Table S2. Symbols used for the description of different types of sludge.

Sludge	Description
Feed	Waste activated sludge drawn from the Shahu wastewater treatment plants, without any pretreatment
Seed	Anaerobic digestion sludge obtained from the Sanjintan wastewater treatment plants, without any pretreatment
Control	The mixture of feed sludge and seed sludge, without any pretreatment
Control30	The mixture of feed sludge and seed sludge exposed to a digestion period of 30 days
UL30	Feed sludge pretreated with ultrasonic intensity of 1.5 W/mL, mixed with seed sludge, and then the mixture was exposed to a digestion period of 30 days
TH30	Feed sludge pretreated at 120 ^{o}C, mixed with seed sludge, and then the mixture was exposed to a digestion period of 30 days
AL30	Feed sludge pretreated at pH of 10, mixed with seed sludge, and then the mixture was exposed to a digestion period of 30 days

Table S3. Band assignments for the protein secondary structures in the liquid phase of different sludge samples.

Protein secondary structure	Wavelength (cm^{-1})	Before anaerobic digestion (Control)	After an incubation of 30 days			
			Control (Control30)	Ultrasonic (UL30)	Thermal (TH30)	Alkaline (AL30)
Aggregated strands (%)	1625−1610	9.2683	9.5977	10.3945	9.9740	21.7961
β−sheet (%)	1640−1630	22.6877	13.6895	13.1228	19.9323	13.1862
Random coil (%)	1645−1640	15.8224	16.0711	17.0312	15.1634	13.2094
α−helix (%)	1657−1648	20.0152	18.6556	19.7141	16.2692	17.0385
3−turnhelix (%)	1666−1659	15.3398	20.1185	18.4769	15.5225	17.2258
Antiparallel β−sheet/aggregated strands (%)	1695−1680	16.8666	21.8677	21.2605	19.1385	17.5439

Table S4. The comparison of methane producing kinetics during anaerobic digestion of the different pretreated sludge samples.

Pre−treatment	Sample	P (mL/g VS)	R_{max} (mL/(g VS·h))	Statistics	
				Reduced Chi−Sqr	R^2
Control	30	40.06	0.16	4.40	0.98
Temperature (°C)	30	57.86	0.17	11.14	0.97
	60	60.91	0.17	15.82	0.97
	90	71.35	0.18	20.84	0.97
	120	84.21	0.24	4.26	0.99
Ultrasonic (W/mL)	0.2	50.69	0.15	7.65	0.98
	0.4	52.05	0.14	4.89	0.99
	1	56.06	0.18	8.68	0.98
	1.5	65.89	0.19	14.21	0.97
pH	2	74.38	0.19	9.70	0.99
	4	66.79	0.17	7.73	0.99
	7	66.89	0.17	7.92	0.99
	10	77.80	0.21	3.88	0.99

Table S5. The relative abundance of main microbes responsible for the degradation of proteins and amino acids at the genus level (%).

Genus	Sludge sample		Control	After an incubation of 30 days			
	Feed	Seed		Control30	UL30	TH30	AL30
Proteiniphilum	0.00291	0.00331	0.00323	0.00399	0.00418	0.00770	0.00431
Tissierella	0.000279	0.00128	0.000721	0.00236	0.00225	0.00270	0.00239

Table S6. The relative abundance (%) of key genes involved in amino acid metabolism in different sludge samples (% denotes the percentage of each gene to the total genes).

Key genes	After an incubation of 30 days				Description
	Control30	UL30	TH30	AL30	
K02500	0.0207	0.0207	0.0225	0.0210	Alanine, aspartate and glutamate metabolism
K02600	0.0282	0.0288	0.0289	0.0291	Glycine, serine and threonine metabolism
K00280	0.0000	0.0000	0.0000	0.0000	Valine, leucine and isoleucine degradation
K00281	0.0121	0.0119	0.0113	0.0114	Geraniol degradation
K00290	0.0019	0.0021	0.0027	0.0020	Valine, leucine and isoleucine biosynthesis
K03100	0.0337	0.0338	0.0357	0.0345	Lysine degradation
K00330	0.0151	0.0166	0.0143	0.0148	Arginine and proline metabolism
K00340	0.0153	0.0159	0.0142	0.0151	Histidine metabolism
K00350	0.0044	0.0042	0.0055	0.0045	Tyrosine metabolism
K03600	0.0017	0.0019	0.0014	0.0016	Phenylalanine metabolism
K00380	0.0010	0.0010	0.0011	0.0010	Tryptophan metabolism
K00400	0.0029	0.0025	0.0037	0.0030	Phenylalanine, tyrosine and tryptophan biosynthesis
K00410	0.0001	0.0001	0.0001	0.0001	beta−Alanine metabolism
K00440	0.0014	0.0012	0.0016	0.0015	Phosphonate and phosphinate metabolism
K00450	0.0008	0.0008	0.0009	0.0008	Selenocompound metabolism
K00471	0.0002	0.0002	0.0002	0.0003	D−Glutamine and D−glutamate metabolism
K00472	0.0007	0.0009	0.0007	0.0007	D−Arginine and D−ornithine metabolism
K00480	0.0010	0.0011	0.0008	0.0009	Glutathione metabolism
Sum	0.1409	0.1436	0.1454	0.1423	

Table S7. The theoretical and measured methane volume and the related methane yields of anaerobic sludge digestion while different concentrations of cysteine were added.

Cysteine concentration (mg/L)	0	20	40	60	80	100
Initial total COD concentration (g/L)	19.36	19.36	19.36	19.36	19.36	19.36
Final total COD concentration (g/L)	18.55	18.02	17.90	17.76	17.96	17.83
Theoretically calculated volume of methane production (mL)*	56.88	93.62	102.28	111.69	98.01	107.28
The measured volume of methane production (mL)	69.08	77.23	77.62	86.04	81.13	80.72
Theoretically methane production yield (mL/day)*	11.38	18.73	20.46	22.34	19.60	21.46
The measured methane production yield (mL/day)	13.82	15.45	15.52	17.21	16.23	16.14

*denotes the theoretically produced methane volume was calculated based on the assumption that 1 g COD equals to 0.35 L methane.

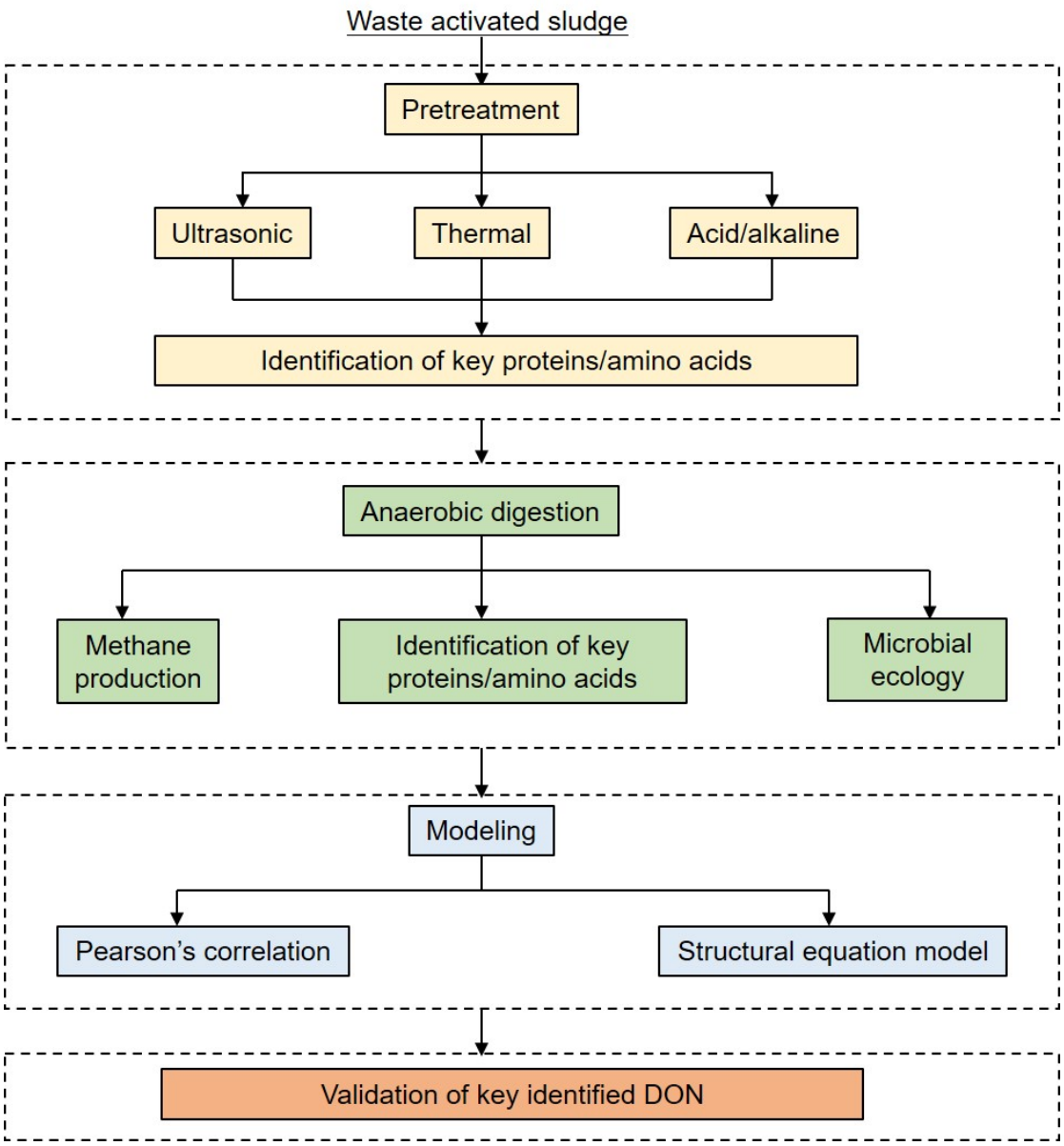

Fig. S1. Schematic of this study.

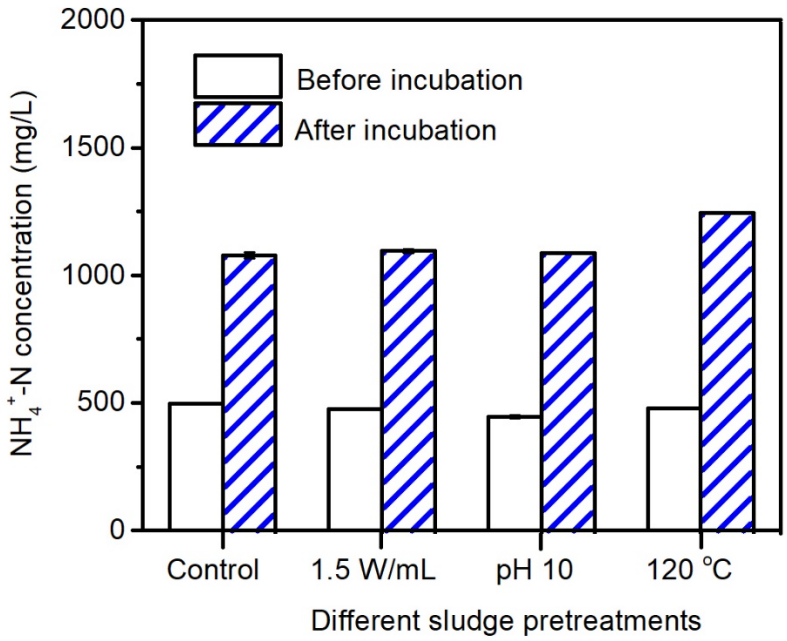

Fig. S2. The changes of NH_4^+-N concentrations in the supernatant of sludge samples in control group, and sludge samples pretreated with ultrasonic intensity of 1.5 W/mL, alkaline at pH of 10, and temperature of 120 °C before and after a digestion period of 30 days.

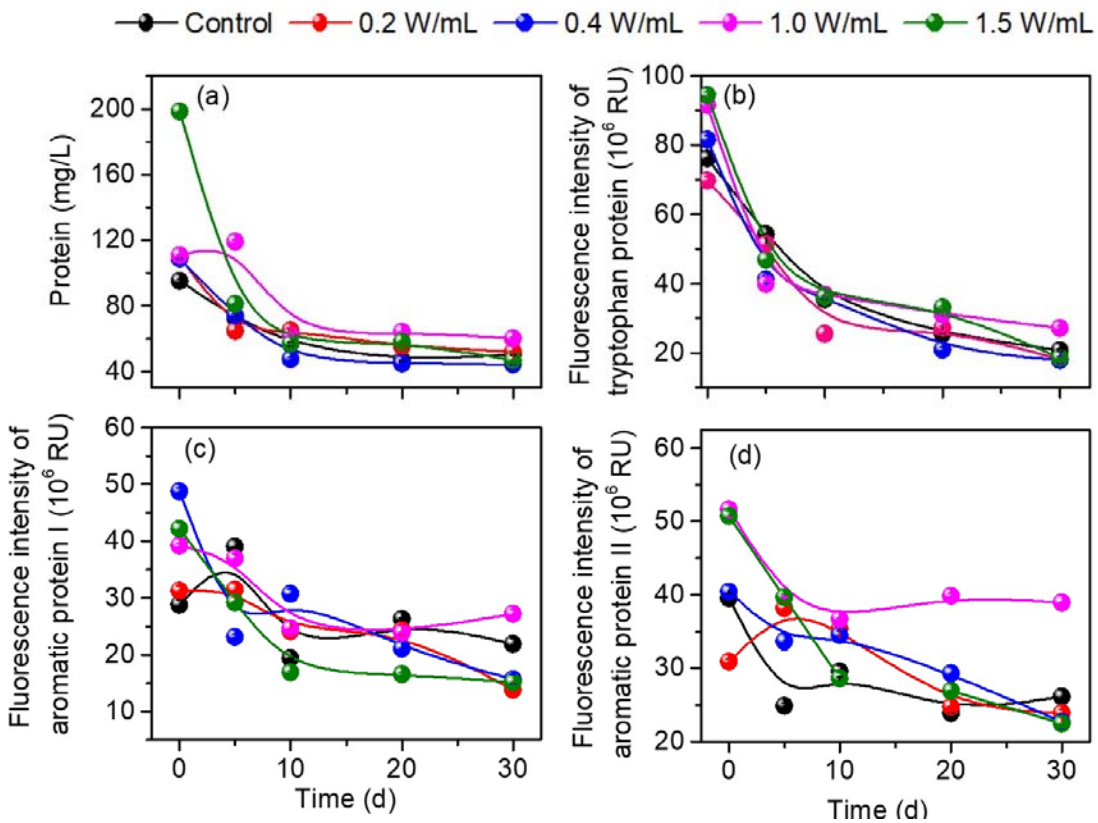

Fig. S3. The changes of protein contents by ultrasonic pretreatment: (a) total protein concentration, (b) the fluorescence intensity of tryptophan protein, (c) the fluorescence intensity of aromatic protein I, and (d) the fluorescence intensity of aromatic protein II.

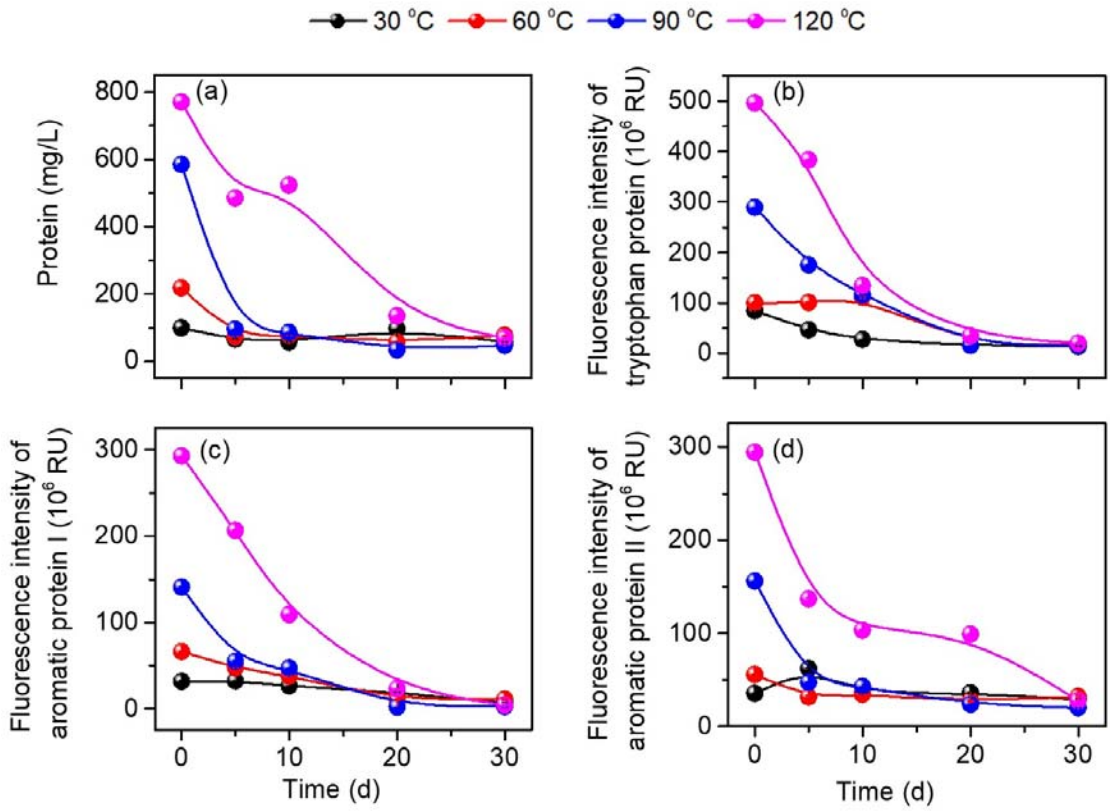

Fig. S4. The changes of protein contents by thermal pretreatment: (a) total protein concentration, (b) the fluorescence intensity of tryptophan protein, (c) the fluorescence intensity of aromatic protein I, and (d) the fluorescence intensity of aromatic protein II.

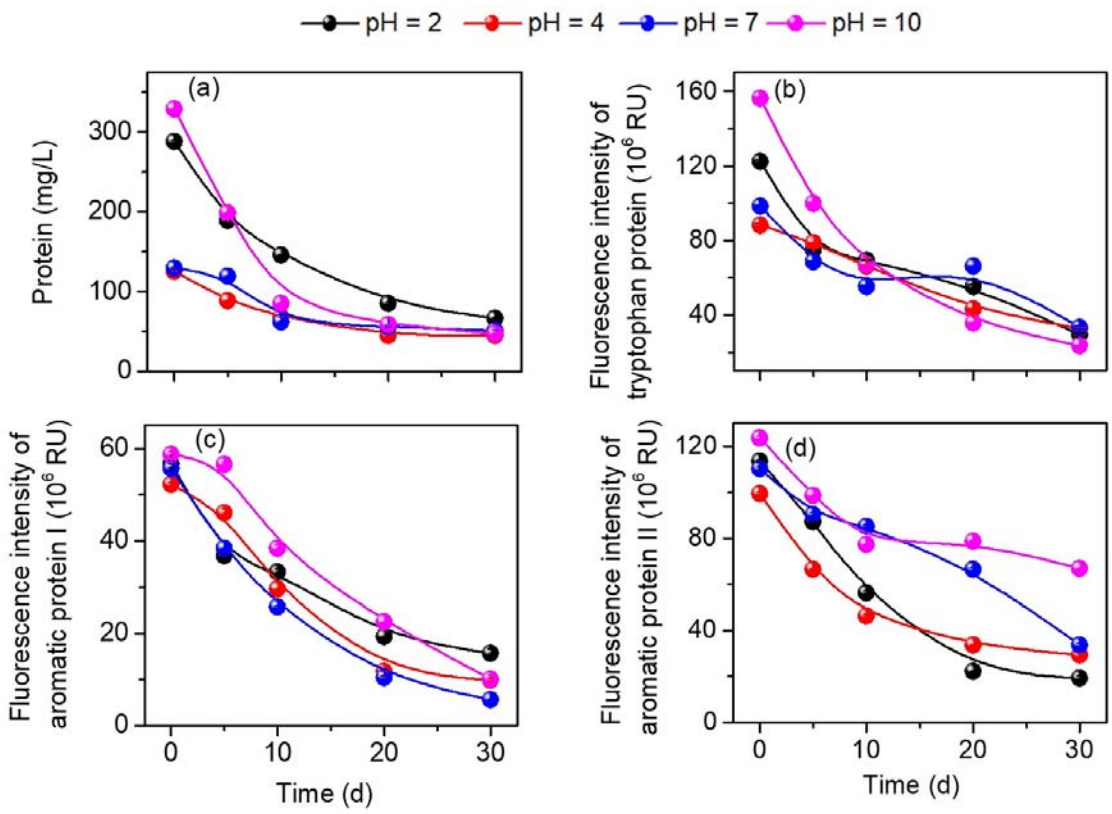

Fig. S5. The changes of protein contents by acid/alkaline pretreatment: (a) total protein concentration, (b) the fluorescence intensity of tryptophan protein, (c) the fluorescence intensity of aromatic protein I, and (d) the fluorescence intensity of aromatic protein II.

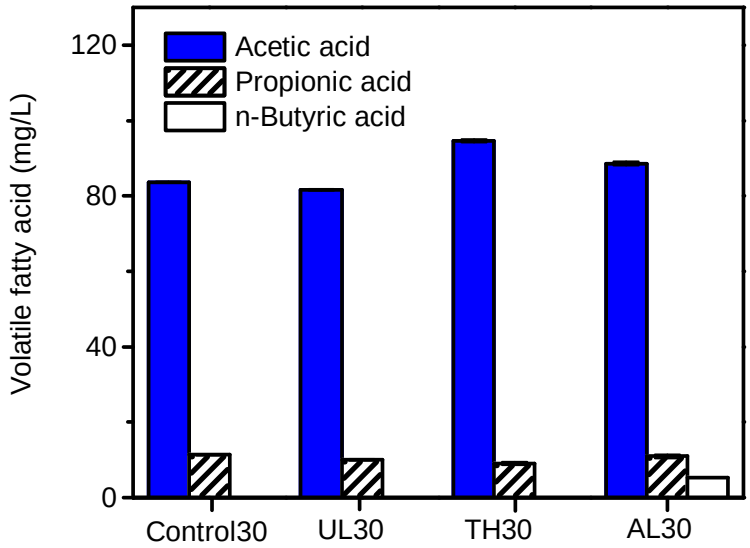

Fig. S6. The changes of volatile fatty acids concentrations in different sludge samples.

References

Apha (2005). Standard methods for the examination for water and wastewater, 21st ed. American Public Health Association: Washington, D.C.

Bäckhed F, Roswall J, Peng Y, Feng Q, Jia H, Kovatcheva-Datchary P, Li Y, Xia Y, Xie H, Zhong H, Khan Muhammad t, Zhang J, Li J, Xiao L, Al-Aama J, Zhang D, Lee Ying s, Kotowska D, Colding C, Tremaroli V, Yin Y, Bergman S, Xu X, Madsen L, Kristiansen K, Dahlgren J, Wang J (2015). Dynamics and stabilization of the human gut microbiome during the first year of life. Cell Host & Microbe, 17(5): 690-703

Berg J, Brandt K K, Al-Soud W A, Holm P E, Hansen L H, Sørensen S J, Nybroe O (2012). Selection for Cu-tolerant bacterial communities with altered composition, but unaltered richness, via long-term Cu exposure. Applied Environmetal Microbiology, 78(20): 7438-7446

Cantarel B L, Coutinho P M, Rancurel C, Bernard T, Lombard V, Henrissat B (2009). The Carbohydrate-Active EnZymes database (CAZy): an expert resource for Glycogenomics. Nucleic Acids Research, 37(1): 233-238

Fei X, Zekkos D, Raskin L (2015). Archaeal community structure in leachate and solid waste is correlated to methane generation and volume reduction during biodegradation of municipal solid waste. Waste Management, 36(1): 184-190

Feng Q, Liang S, Jia H, Stadlmayr A, Tang L, Lan Z, Zhang D, Xia H, Xu X, Jie Z, Su L, Li X, Li X, Li J, Xiao L, Huber-Schönauer U, Niederseer D, Xu X, Al-Aama J Y, Yang H, Wang J, Kristiansen K, Arumugam M, Tilg H, Datz C, Wang J (2015). Gut microbiome development along the colorectal adenoma–carcinoma sequence. Nature Communications, 6(1): 6528

Handelsman J, Rondon M R, Brady S F, Clardy J, Goodman R M (1998). Molecular biological access to the chemistry of unknown soil microbes: a new frontier for natural products. Chemistry & Biology, 5(10): 245-249

Kanehisa M, Goto S, Hattori M, Aoki-Kinoshita K F, Itoh M, Kawashima S, Katayama T, Araki M, Hirakawa M

(2006). From genomics to chemical genomics: new developments in KEGG. Nucleic Acids Research, 34(1): 354-357

Kanehisa M, Goto S, Sato Y, Kawashima M, Furumichi M, Tanabe M (2013). Data, information, knowledge and principle: back to metabolism in KEGG. Nucleic Acids Research, 42(1): 199-205

Karlsson F H, Fåk F, Nookaew I, Tremaroli V, Fagerberg B, Petranovic D, Bäckhed F, Nielsen J (2012). Symptomatic atherosclerosis is associated with an altered gut metagenome. Nature Communications, 3(1): 1245

Le C C, Stuckey D C (2017). Impact of feed carbohydrates and nitrogen source on the production of soluble microbial products (SMPs) in anaerobic digestion. Water Research, 122(1): 10-16

Li J, Jia H, Cai X, Zhong H, Feng Q, Sunagawa S, Arumugam M, Kultima J R, Prifti E, Nielsen T, Juncker A S, Manichanh C, Chen B, Zhang W, Levenez F, Wang J, Xu X, Xiao L, Liang S, Zhang D, Zhang Z, Chen W, Zhao H, Al-Aama J Y, Edris S, Yang H, Wang J, Hansen T, Nielsen H B, Brunak S, Kristiansen K, Guarner F, Pedersen O, Doré J, Ehrlich S D, Pons N, Le Chatelier E, Batto J-M, Kennedy S, Haimet F, Winogradski Y, Pelletier E, Lepaslier D, Artiguenave F, Bruls T, Weissenbach J, Turner K, Parkhill J, Antolin M, Casellas F, Borruel N, Varela E, Torrejon A, Denariaz G, Derrien M, Van Hylckama Vlieg J E T, Viega P, Oozeer R, Knoll J, Rescigno M, Brechot C, M'rini C, Mérieux A, Yamada T, Tims S, Zoetendal E G, Kleerebezem M, De Vos W M, Cultrone A, Leclerc M, Juste C, Guedon E, Delorme C, Layec S, Khaci G, Van De Guchte M, Vandemeulebrouck G, Jamet A, Dervyn R, Sanchez N, Blottière H, Maguin E, Renault P, Tap J, Mende D R, Bork P, Wang J, Meta H I T C (2014). An integrated catalog of reference genes in the human gut microbiome. Nature Biotechnology, 32(8): 834-841

Li Y, Chen Y G, Wu J (2019). Enhancement of methane production in anaerobic digestion process: A review. Applied Energy, 240(2): 120-137

Nielsen H B, Almeida M, Juncker A S, Rasmussen S, Li J, Sunagawa S, Plichta D R, Gautier L, Pedersen A G, Le Chatelier E, Pelletier E, Bonde I, Nielsen T, Manichanh C, Arumugam M, Batto J-M, Quintanilha Dos Santos M B,

Blom N, Borruel N, Burgdorf K S, Boumezbeur F, Casellas F, Doré J, Dworzynski P, Guarner F, Hansen T, Hildebrand F, Kaas R S, Kennedy S, Kristiansen K, Kultima J R, Léonard P, Levenez F, Lund O, Moumen B, Le Paslier D, Pons N, Pedersen O, Prifti E, Qin J, Raes J, Sørensen S, Tap J, Tims S, Ussery D W, Yamada T, Nielsen H B, Almeida M, Juncker A S, Rasmussen S, Li J, Sunagawa S, Plichta D R, Gautier L, Pedersen A G, Le Chatelier E, Pelletier E, Bonde I, Nielsen T, Manichanh C, Arumugam M, Batto J-M, Quintanilha Dos Santos M B, Blom N, Borruel N, Burgdorf K S, Boumezbeur F, Casellas F, Doré J, Dworzynski P, Guarner F, Hansen T, Hildebrand F, Kaas R S, Kennedy S, Kristiansen K, Kultima J R, Leonard P, Levenez F, Lund O, Moumen B, Le Paslier D, Pons N, Pedersen O, Prifti E, Qin J, Raes J, Sørensen S, Tap J, Tims S, Ussery D W, Yamada T, Renault P, Sicheritz-Ponten T, Bork P, Wang J, Brunak S, Ehrlich S D, Jamet A, Mérieux A, Cultrone A, Torrejon A, Quinquis B, Brechot C, Delorme C, M'rini C, De Vos W M, Maguin E, Varela E, Guedon E, Gwen F, Haimet F, Artiguenave F, Vandemeulebrouck G, Denariaz G, Khaci G, Blottière H, Knol J, Weissenbach J, Van Hylckama Vlieg J E T, Torben J, Parkhill J, Turner K, Van De Guchte M, Antolin M, Rescigno M, Kleerebezem M, Derrien M, Galleron N, Sanchez N, Grarup N, Veiga P, Oozeer R, Dervyn R, Layec S, Bruls T, Winogradski Y, Erwin G Z, Renault P, Sicheritz-Ponten T, Bork P, Wang J, Brunak S, Ehrlich S D, Meta H I T C (2014). Identification and assembly of genomes and genetic elements in complex metagenomic samples without using reference genomes. Nature Biotechnology, 32(8): 822-828

Powell S, Forslund K, Szklarczyk D, Trachana K, Roth A, Huerta-Cepas J, Gabaldón T, Rattei T, Creevey C, Kuhn M, Jensen L J, Von Mering C, Bork P (2014). eggNOG v4.0: nested orthology inference across 3686 organisms. Nucleic Acids Research, 42(1): 231-239

Tringe S G, Rubin E M (2005). Metagenomics: DNA sequencing of environmental samples. Nature Reviews Genetics, 6(11): 805-814

Tringe S G, Von Mering C, Kobayashi A, Salamov A A, Chen K, Chang H W, Podar M, Short J M, Mathur E J,

Detter J C, Bork P, Hugenholtz P, Rubin E M (2005). Comparative metagenomics of microbial communities. Science, 308(5721): 554-557

Xiao K K, Chen Y, Jiang X, Seow W Y, He C, Yin Y, Zhou Y (2017). Comparison of different treatment methods for protein solubilisation from waste activated sludge. Water Research, 122(1): 492-502

Xiao K K, Chen Y, Jiang X, Tyagi V K, Zhou Y (2016). Characterization of key organic compounds affecting sludge dewaterability during ultrasonication and acidification treatments. Water Research, 105(2): 470-478

You G X, Wang P F, Hou J, Wang C, Xu Y, Miao L Z, Lv B W, Yang Y Y, Liu Z L, Zhang F (2017). Insights into the short-term effects of CeO_2 nanoparticles on sludge dewatering and related mechanism. Water Research, 118(3): 93-103

Zong F, Yu P, Tang J J, Su X (2019). Understanding parking decisions with structural equation modeling. Physica a-Statistical Mechanics and Its Applications, 523(4): 408-417